Clinical Pharmacokinetics

Supplementary Information

COMPARATIVE PLASMA AND INTERSTITIAL TISSUE FLUID PHARMACOKINETICS OF MEROPENEM DEMONSTRATE THE NEED FOR INCREASING DOSE AND INFUSION DURATION IN OBESE AND NON-OBESE PATIENTS

D. Busse*, P. Simon*, L. Schmitt, D. Petroff, C. Dorn, A. Dietrich, M. Zeitlinger, W. Huisinga, R. Michelet, H. Wrigge, C. Kloft

* Contributed equally

Corresponding author:

Charlotte Kloft. Prof. Dr.

Department of Pharmacy, Freie Universitaet Berlin,

Kelchstr. 31

12169 Berlin, Germany

Phone +49 30 838 50676

Email charlotte.kloft@fu-berlin.de

Table S1 Summary of model-evaluated dosing regimens of meropenem.

Daily dose [mg]	Short-term infusion over 30 min	Prolonged infusion over 3 h	Continuous infusion over 24 h
3000 or 4000[1]	1000 mg q8h	1000 mg q8h	3000 mg q24h following initial loading dose of 1000 mg over 30 min
6000 or 7000[1]	2000 mg q8h	2000 mg q8h	6000 mg q24h following initial loading dose of 1000 mg over 30 min

[1]For continuous infusion treatment at day 1, the initial loading dose is included;
Abbreviations: *q8h* every 8 hours, *q12h* every 12 hours, *q24h* every 24 hours

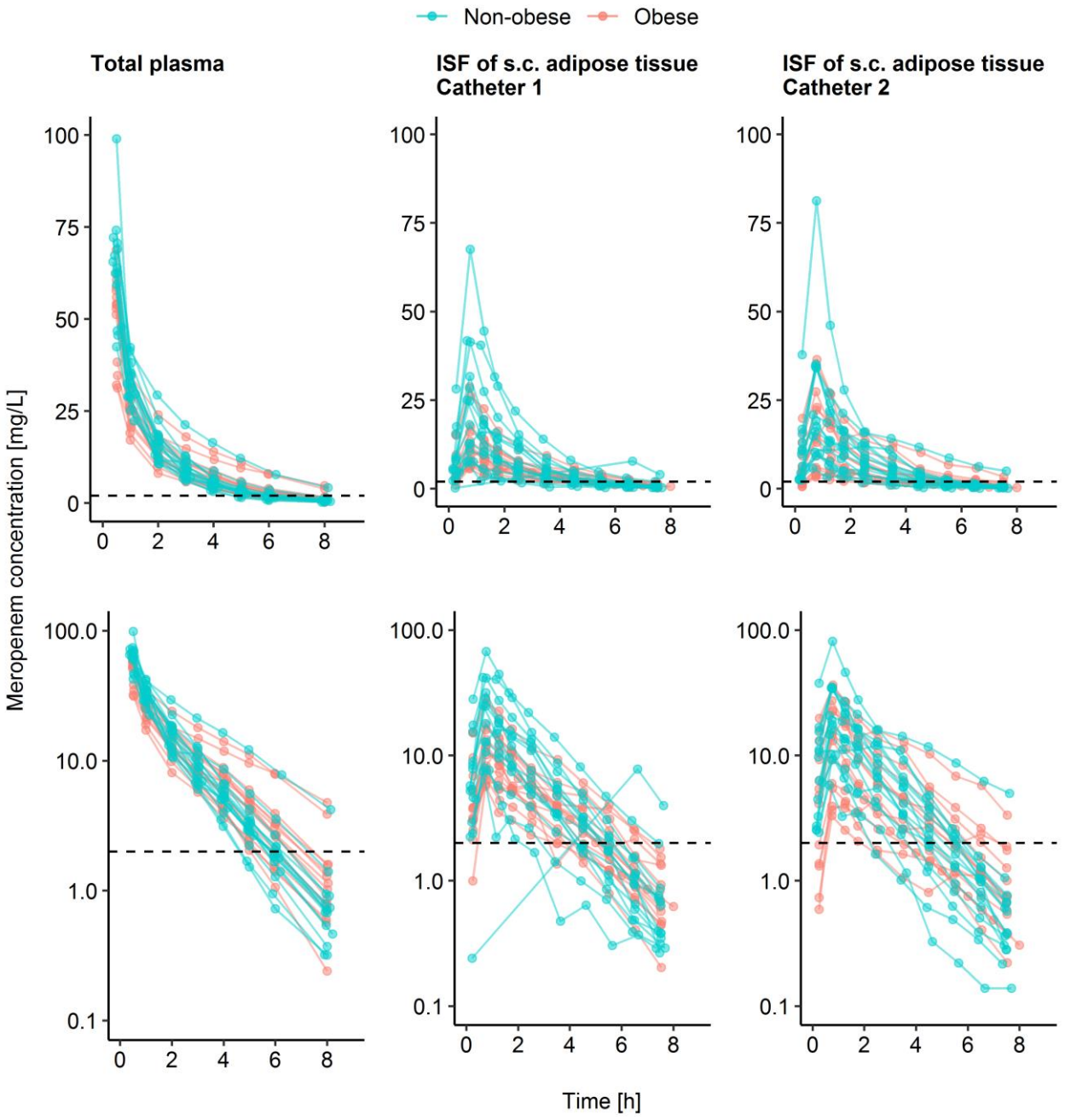

Fig. S1 Observed individual meropenem concentration-time profiles in plasma (total concentration) and interstitial space fluid (ISF) of subcutaneous (s.c.) adipose tissue for both catheters (unbound concentration) for obese (n=15) and non-obese patients (n=15). ISF concentrations are displayed at the mid-time of the respective collection intervals. Dashed line: MIC=2 mg/L.

Population pharmacokinetic model development

Key steps in the population pharmacokinetic model development are outlined in Table S2. To quantify the impact of different body size descriptors on drug distribution and elimination, allometric scaling was applied [1]. The allometric exponent was either (i) fixed to 1 for volumes and 0.75 for flows or (ii) estimated separately for all flows and volumes (i.e. estimation of two exponents in the model). For the selected body size descriptor, adjusted body weight (ABW), exponents were also estimated separately for all PK parameters (i.e. one for each structural PK parameter). This model development step resulted in inadequate parameter precision (RSE≥50%) for the exponents associated with both intercompartmental flows (Q_1 and Q_2) and the volume of distribution associated with the "deep" compartment (V_3, compare to Fig. 2 and Table 2 in the main manuscript).

Subsequently, the allometric scaling of those parameters that showed poor precision of exponent estimates (i.e. Q_1, Q_2 and V_3) were omitted and only the exponents associated with clearance (CL), and the central and "shallow" peripheral volume of distribution (V_1 and V_2, compare to Fig. 2 and Table 2 in the main manuscript) were estimated. These omissions allowed the estimation of these 3 remaining exponents with adequate parameter precision (RSE<50%). Yet, no significant decrease of the AIC compared to the model with fixed exponents ($AIC_{fixed\ exponents}$-$AIC_{estimated\ exponents}$=-0.98) was achieved (Fig. S2).

This means, these estimated exponents did not improve the prediction of the observed concentrations, and hence there is no justification of including these additional estimated exponent parameters into the model. Furthermore, the confidence intervals of the estimated exponent values ($Exponent_{CL}$=0.512, 95%CI=[0.144, 0.912]; $Exponent_{V1}$=1.03, 95%CI=[0.560, 1.88]; $Exponent_{V2}$=1.15, 95%CI=[0.433, 1.90]) all included the fixed exponents (0.75 for flows and 1 for volumes). Additionally, deviations of structural PK parameter estimates between the model with estimated exponents and fixed exponents were relatively small ($\leq$|13.3%| for all PK parameters except for Q_2 with +51.3%), demonstrating a lack of bias in PK parameters when fixing exponents in allometric scaling. In conclusion, a more empirical covariate PK model did not result in an improvement of the model.

Table S2 Key models in the population pharmacokinetic model development.

Development step	Model description	AIC	Selection
Structural model	2-CMT model, ISF associated with peripheral CMT	400	
	2-CMT model, ISF associated with central CMT	732	
	3-CMT mammillary model, ISF associated with peripheral CMT	379	
	3-CMT serial model, ISF associated with "shallow" peripheral CMT	346	x
Impact of body size descriptors on drug distribution and elimination (investigated via allometric scaling)	Ideal body weight, fixed exponents	342	
	estimated exponents	338	
	Lean body weight, fixed exponents	304	
	estimated exponents	304	
	Total body weight, fixed exponents	326	
	estimated exponents	293	
	Body mass index, fixed exponents	328	
	estimated exponents	293	
	Adjusted body weight, fixed exponents	293	x
	estimated exponents[1]	292	
	estimated exponents all PK parameters[2]	289	
	estimated exponents selected parameters[3]	292	
	Residual fat mass	305	
Mechanism-based elimination: CL split into CL_{Rfilt} and $CL_{nonfilt}$	CL_{Rfilt} via IBW-based $CLCR_{CG}$	288	
	CL_{Rfilt} via LBW-based $CLCR_{CG}$	286	
	CL_{Rfilt} via TBW-based $CLCR_{CG}$	291	
	CL_{Rfilt} via ABW-based $CLCR_{CG}$	285	x
	CL_{Rfilt} via de-indexed eGFR by MDRD	284	
	CL_{Rfilt} via de-indexed eGFR by CKD-EPI	285	
Impact of anesthesia-related haemodynamic changes on PK parameters	Presence of anesthesia on tissue factor	276	x
	Mean arterial blood pressure on CL_{Rfilt}	273	
	Mean arterial blood pressure on $CL_{nonfilt}$	271	x
Obesity related change in RR	Separate parameter estimates for obese and non-obese patients	253	x
Remaining parameter correlations	Correlations estimated between PK parameters[4]	251	x
Microdialysis/retrodialysis technique variabilities	Logit-normally distributed variability between patients, between catheters and within catheters	30.4	x

[1]Estimated exponents were close to close to fixed exponents (0.757, 90%CI=[0.408, 1.10] for volumes, 0.505, 90%CI=[0.135, 0.876] for flows).

[2]Exponents, estimated separately for each PK parameter, were imprecisely (relative standard error≥50%) estimated for intercompartmental flows and the „deep" volume of distribution.

[3]Selected exponents, which were previously imprecisely estimated (see [2]) were fixed to 0, i.e. no scaling via ABW, hence exponents for all other PK parameters (CL, central and “shallow” volumes of distribution) were estimated separately.
[4]Necessary to describe observed variabilities in microdialysis data adequately.
Abbreviations: *AIC* Akaike information criterion, *CL* meropenem clearance, $CL_{nonfilt}$ CL via processes other than glomerular filtration, CL_{Rfilt} renally filtered part of CL related to $CLCR_{CG\_ABW}$, *CMT* compartment, *ISF* interstitial space fluid of subcutaneous fat tissue, *RR* relative recovery

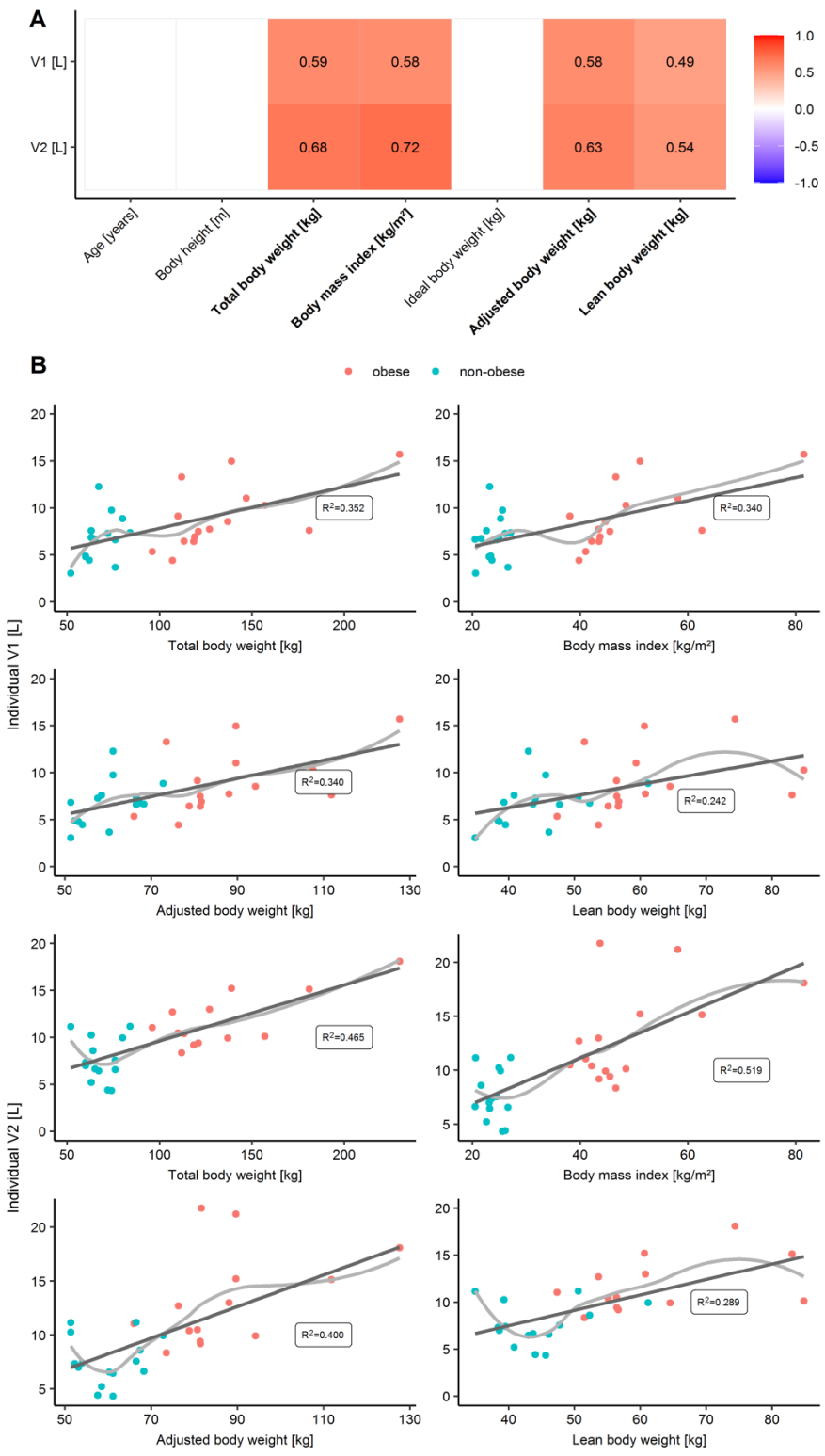

Fig. S2 Individual estimates of volume of distribution before implementation of covariate relationships versus evaluated patient characteristics (A). Pearson´s correlation coefficient is only shown for statistically significant relationships (p<0.01, bold axis labels), which are presented in more detail in B. Black line: Linear regression line; grey line: Loess smoother.
Abbreviations: *V1* central volume of distribution, *V2* peripheral volume of distribution, *R²* coefficient of determination.

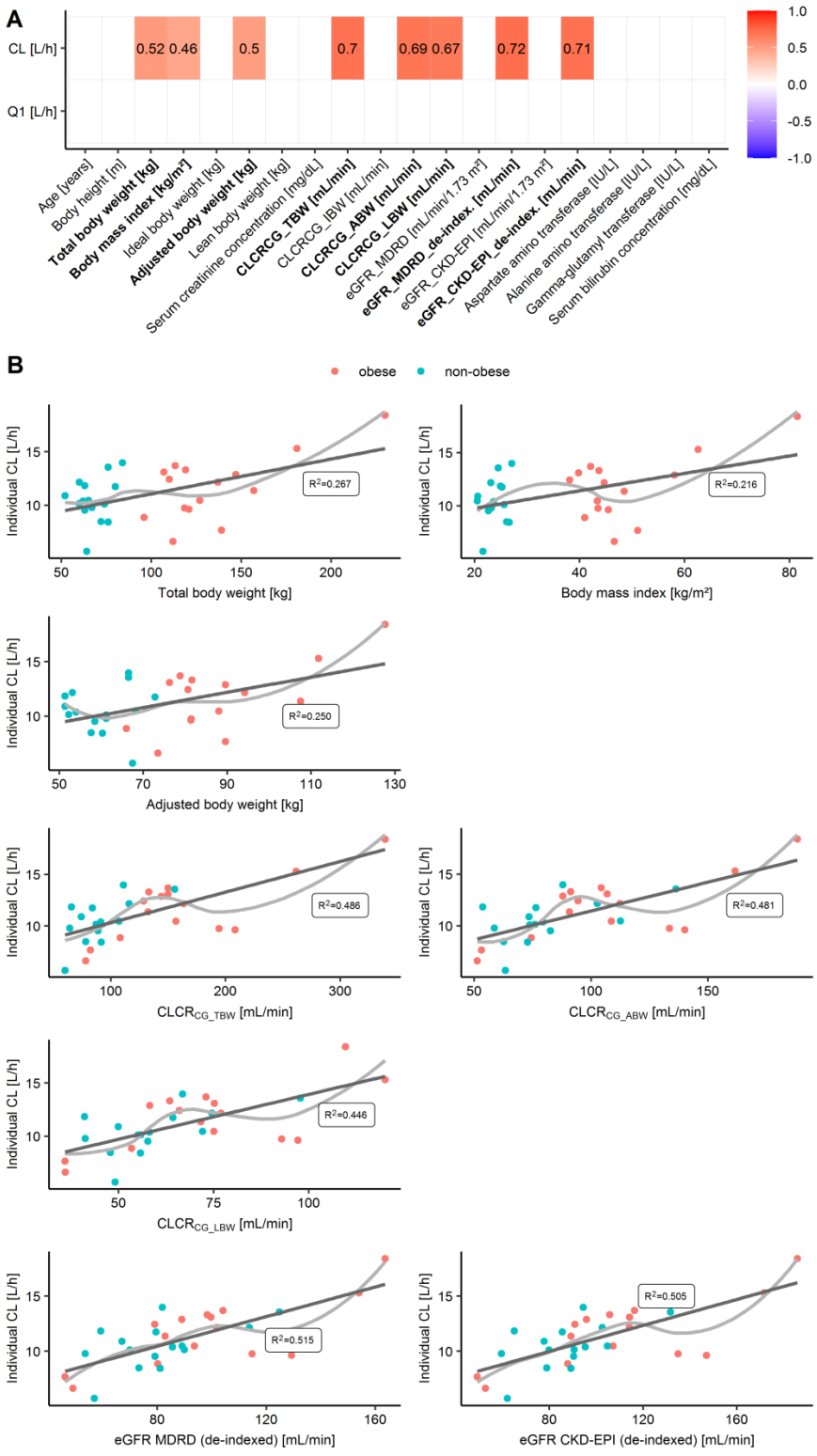

Fig. S3 Individual estimates of flows before implementation of covariate relationships versus evaluated patient characteristics (A). Pearson´s correlation coefficient is only shown for statistically significant relationships (p<0.01, bold axis labels), which are presented in more detail in B. Black line: Linear regression line; grey line: Loess smoother.
Abbreviations: *CL* clearance, *Q1* intercompartmental flow between the central and first peripheral compartment, *R²* coefficient of determination.

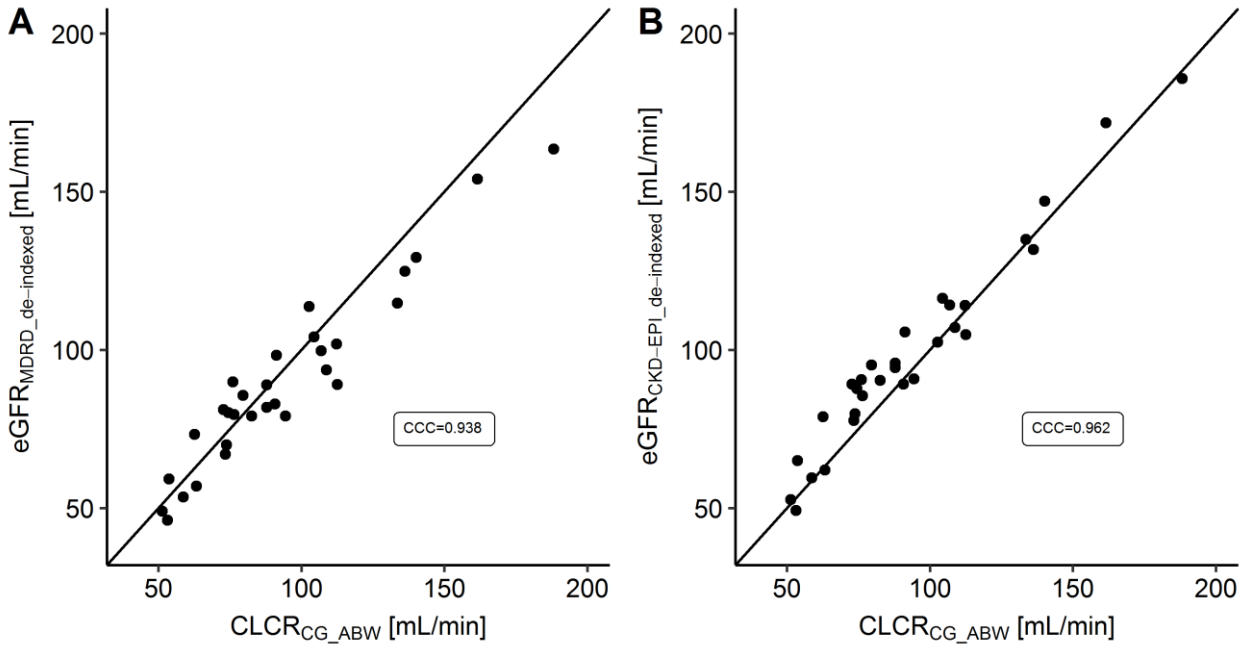

Fig. S4 Concordance between serum creatinine clearance calculated via Cockcroft-Gault equation based on ABW ($CLCR_{CG\_ABW}$) and body surface area de-normalised ("de-indexed") predicted glomerular filtration rate calculated via the MDRD (A, $eGFR_{MDRD\_de\text{-}indexed}$) and via the CKD-EPI formula (B, $eGFR_{CKD\text{-}EPI\_de\text{-}indexed}$).
Points: Observations for the patients of this study (n=30); Line: Line of unity.
Abbreviations: *CCC* Lin´s concordance correlation coefficient, *MDRD* Modification of Diet in Renal Disease, *CKD-EPI* Chronic Kidney Disease Epidemiology Collaboration

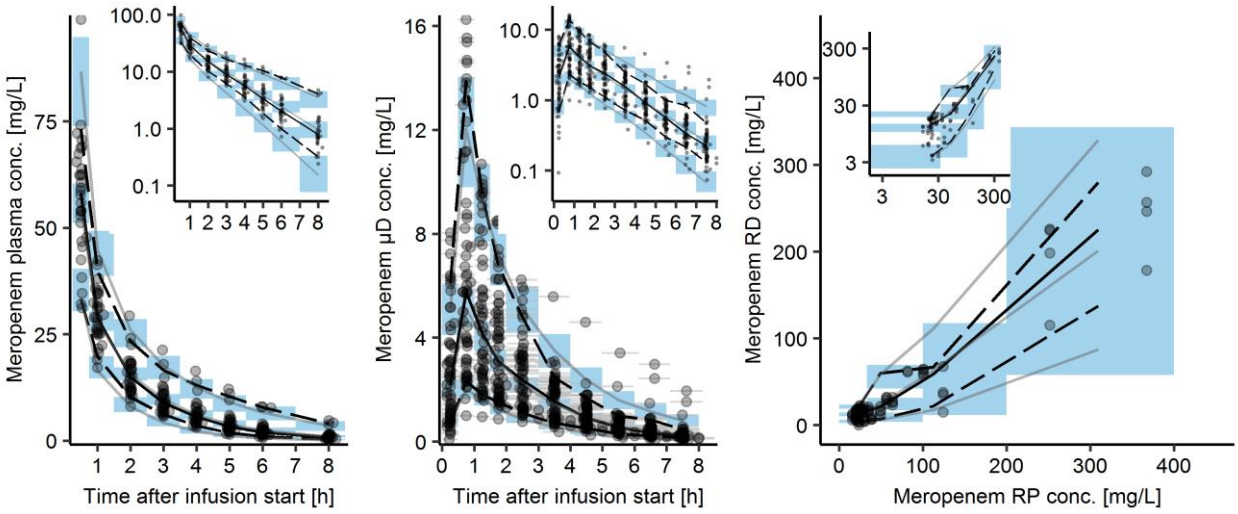

Fig. S5 Visual predictive check (n=1000 simulations) for the final pharmacokinetic model for total plasma concentrations (A), microdialysate concentrations (B), and retrodialysate concentrations (C).
Circles: Observed meropenem concentrations; Lines: 5th, 95th percentile (dashed), 50th percentile (solid) of the observed (black) and simulated (grey) data. Shaded areas: 95% confidence interval around 5th, 50th and 95th percentile of simulated data. Horizontal grey lines: µD collection interval. Plot insets are on semilogarithmic scale (A,B) or log-log scale (C).
Abbreviations: *µD* microdialysate, *conc.* concentration, *RD* retrodialysate, *RP* retroperfusate

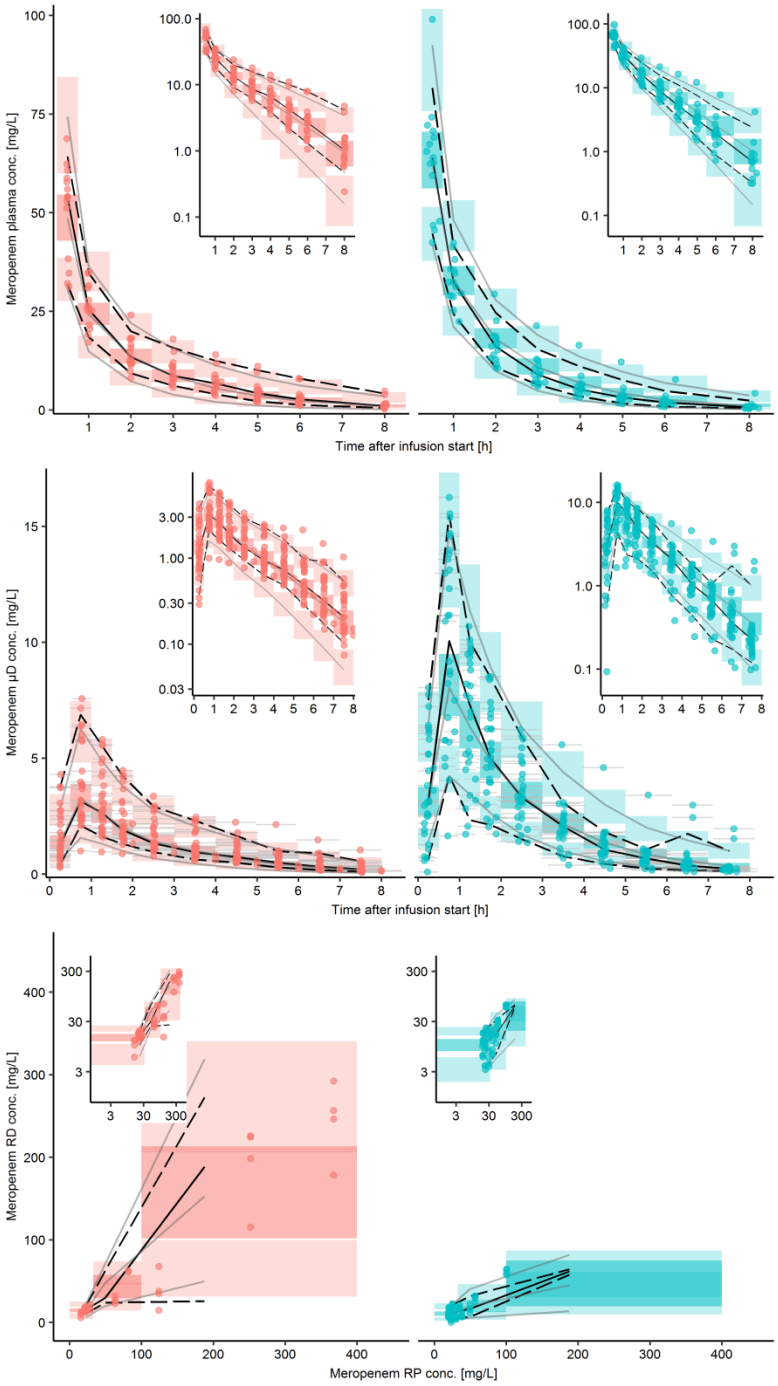

Fig. S6 Visual predictive check (n=1000 simulations) for the final pharmacokinetic model for total plasma concentrations (top panel), microdialysate concentrations (middle panel), and retrodialysate concentrations (bottom panel) for obese (Red) and non-obese patients (Green). Circles: Observed meropenem concentrations; Lines: 5th, 95th percentile (dashed), 50th percentile (solid) of the observed (black) and simulated (grey) data. Shaded areas: 95% confidence interval around 5th, 50th and 95th percentile of simulated data. Horizontal grey lines: µD collection interval. Plot insets are on semilogarithmic scale (A,B) or log-log scale (C).
Abbreviations: *µD* microdialysate, conc. concentration, *RD* retrodialysate, *RP* retroperfusate

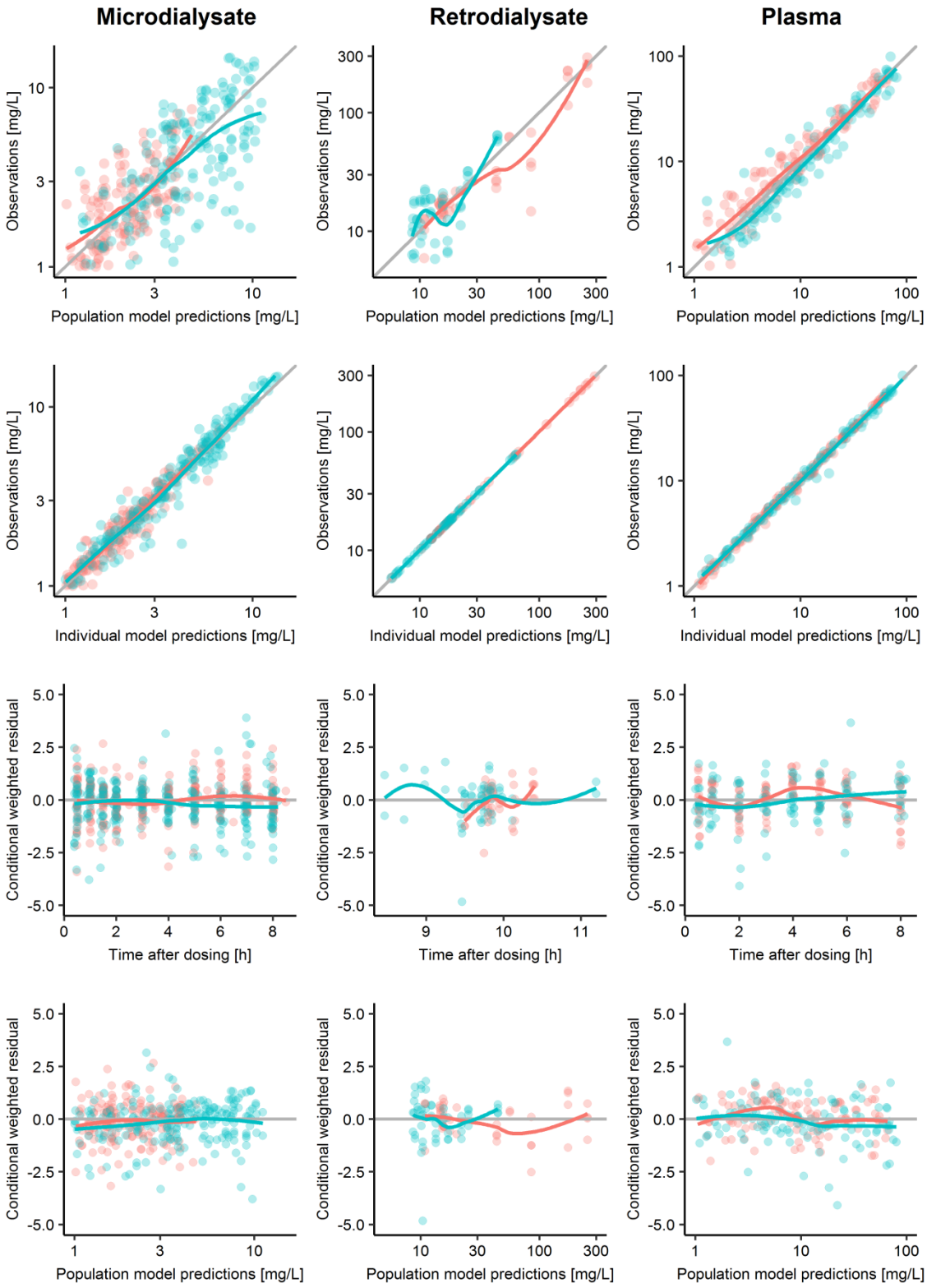

Fig. S7 Basic goodness-of-fit plots with observed and predicted meropenem concentrations on a log-scale for the final pharmacokinetic model for the three matrices: Microdialysate, retrodialysate and plasma. Red dots: obese patients; Green dots: non-obese patients; Grey line: Line of identity; Red line: Loess smoother for obese patients; Green line: Loess smoother for non-obese patients.

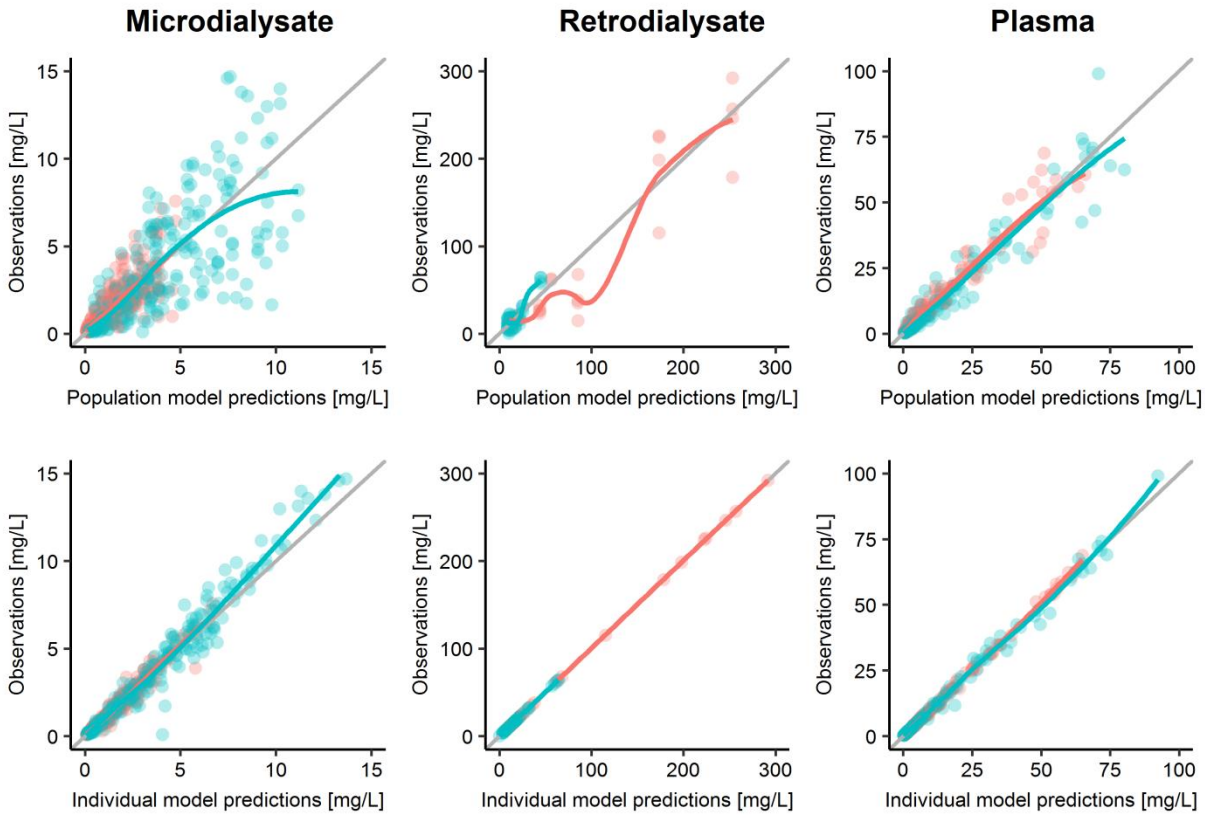

Fig. S8 Basic goodness-of-fit plots with observed and predicted meropenem concentrations on a normal scale for the final pharmacokinetic model for the three matrices: Microdialysate, retrodialysate and plasma. Red dots: obese patients; Green dots: non-obese patients; Grey line: Line of identity; Red line: Loess smoother for obese patients; Green line: Loess smoother for non-obese patients.

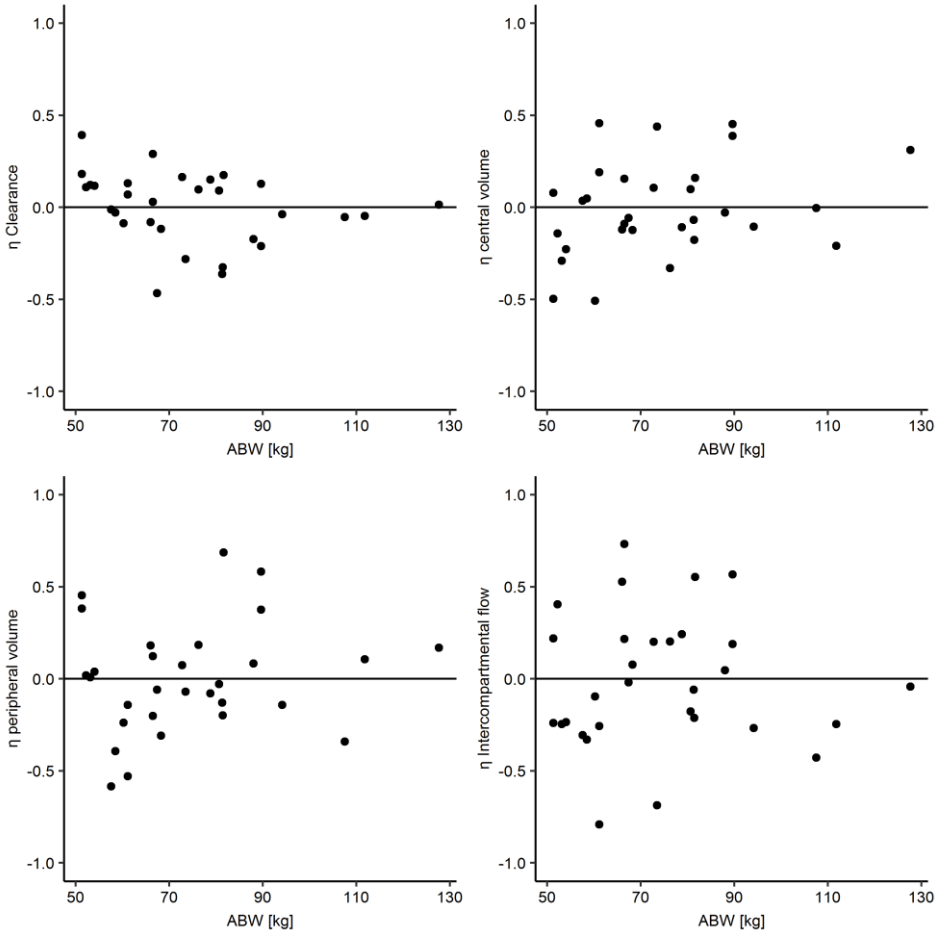

Fig. S9 Random-effects variables (η) for structural pharmacokinetic parameters of the final pharmacokinetic model of meropenem versus adjusted body weight (ABW).

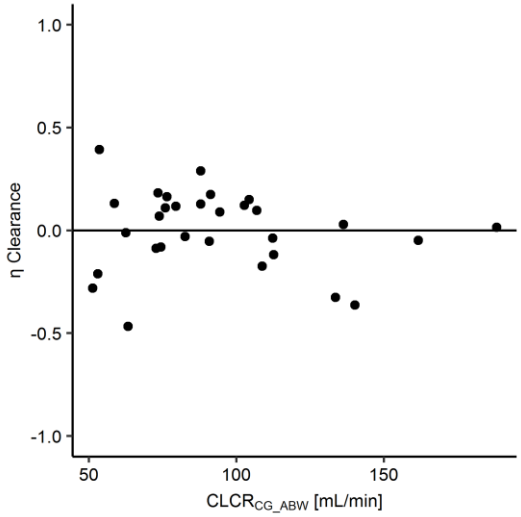

Fig. S10 Random-effects variable (η) for clearance of the final pharmacokinetic model of meropenem versus creatinine clearance calculated via Cockcroft-Gault equation based on adjusted body weight (CLCRCG_ABW).

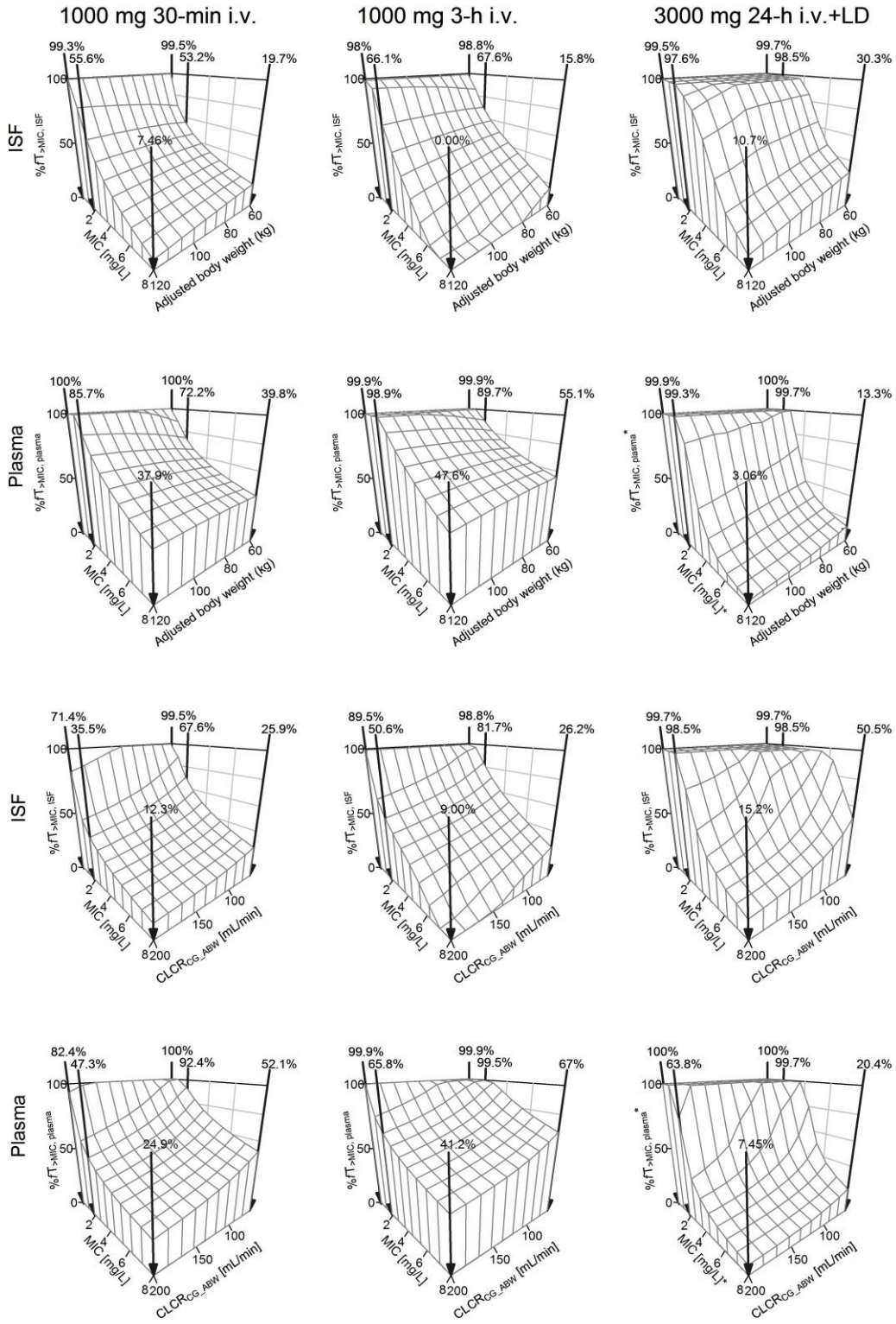

Fig. S11 Percentage of dosing interval time that simulated unbound meropenem concentrations exceeded MIC (%$fT_{>MIC}$) for varying adjusted body weight and creatinine clearance ($CLCR_{CG\_ABW}$) in plasma and in ISF (rows) following three different dosing regimens (panels).

*For continuous infusions %$fT_{>MIC,\ \mathbf{ISF}}$ is related to 1xMIC and %$fT_{>MIC,\ \mathbf{plasma}}$ is related to 4xMIC. **Abbreviations:** *ISF* interstitial space fluid of the subcutaneous adipose tissue, *i.v,* intravenous *MIC* minimum inhibitory concentration, *LD* 1000 mg 30-min i.v. loading dose

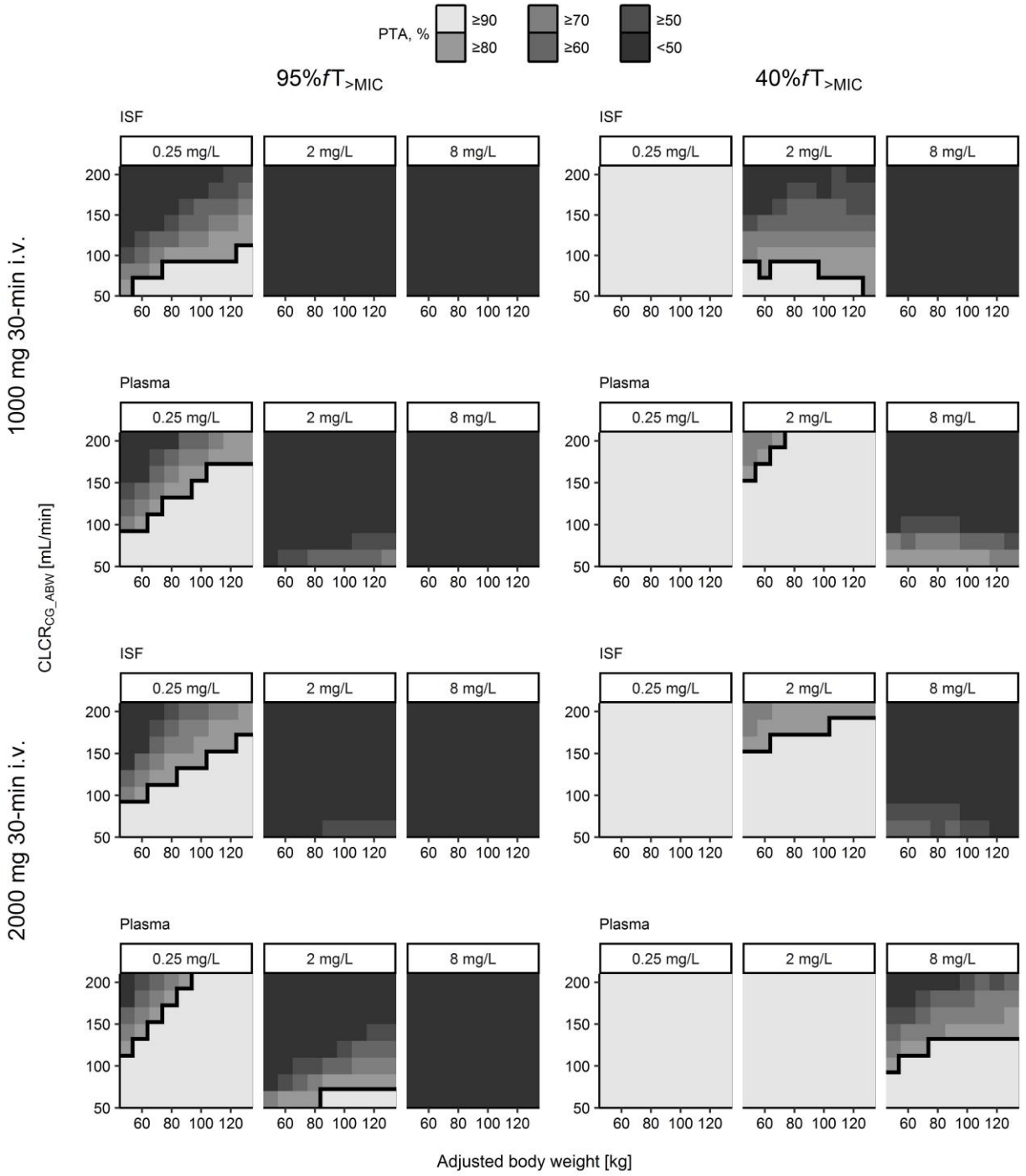

Fig. S12 Probability of target attainment versus adjusted body weight and serum creatinine clearance in plasma and ISF for 1000 mg (top) and 2000 mg (bottom) 30-min **short-term** i.v. infusions thrice daily and 95%$fT_{>MIC}$ (left) 40%$fT_{>MIC}$ (right).

MIC is given at the top of each panel. Bold black lines separate PTA≥90% (adequate therapy, light grey) from PTA<90%.

Abbreviations: *ABW* adjusted body weight, $CLCR_{CG\_ABW}$ serum creatinine clearance calculated via Cockcroft-Gault equation based on ABW, *ISF* interstitial space fluid of the subcutaneous adipose tissue, *i.v,* intravenous, *MIC* minimum inhibitory concentration, *PTA* probability of target attainment, $95\%fT_{>MIC}$/$40\%fT_{>MIC}$ unbound meropenem plasma concentrations exceeding the MIC 95%/40% of the time over 24 h

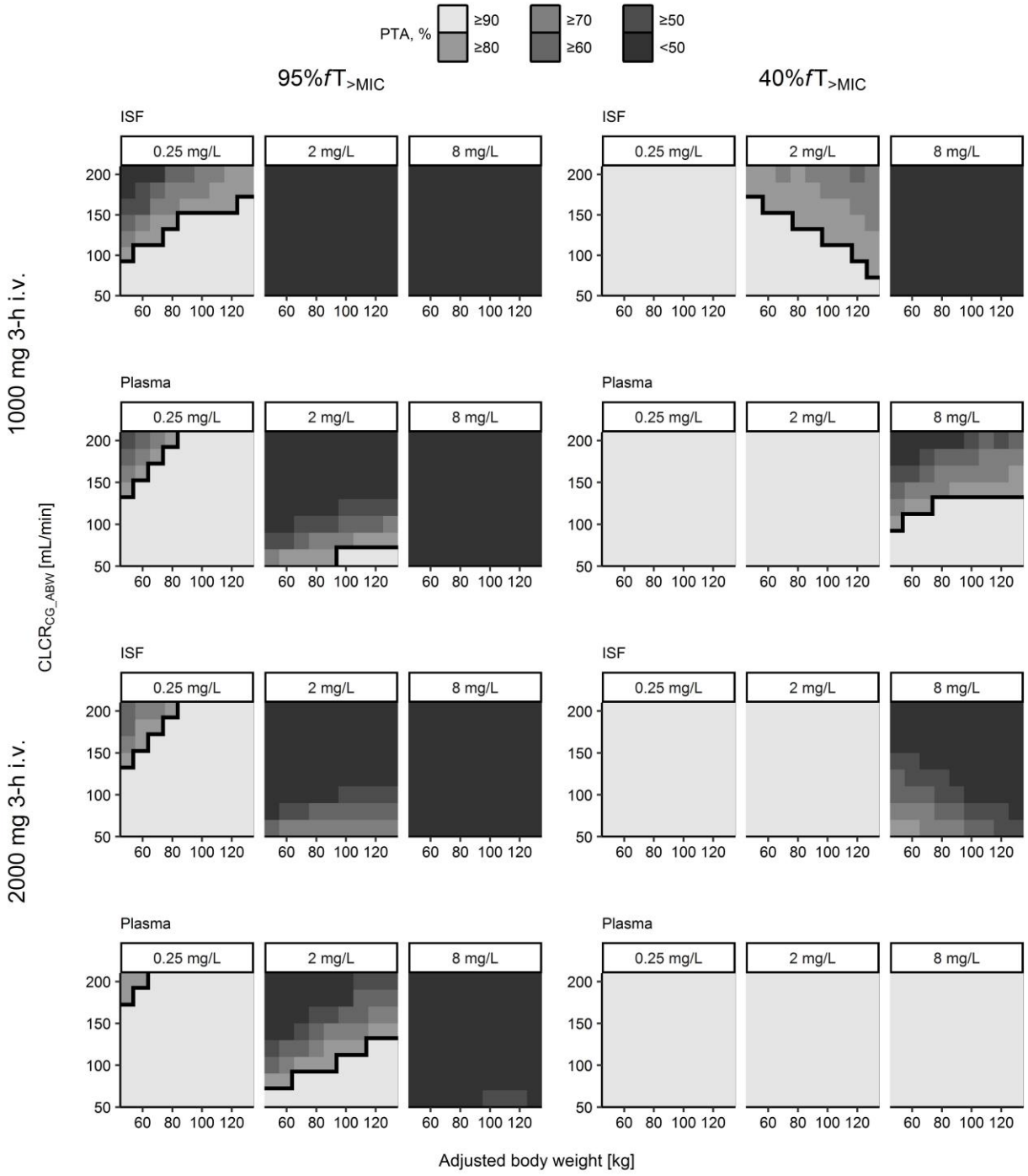

Fig. S13 Probability of target attainment versus adjusted body weight and serum creatinine clearance in plasma and ISF for 1000 mg (top) and 2000 mg (bottom) 3-h **prolonged** i.v. infusions thrice daily and 95%$fT_{>MIC}$ (left) 40%$fT_{>MIC}$ (right).

MIC is given at the top of each panel. Bold black lines separate PTA≥90% (adequate therapy, light grey) from PTA<90%.

Abbreviations: *ABW* adjusted body weight, $CLCR_{CG\_ABW}$ serum creatinine clearance calculated via Cockcroft-Gault equation based on ABW, *ISF* interstitial space fluid of the subcutaneous adipose tissue, *i.v,* intravenous, *MIC* minimum inhibitory concentration, *PTA* probability of target attainment, $95\%fT_{>MIC}/40\%fT_{>MIC}$ unbound meropenem plasma concentrations exceeding the MIC 95%/40% of the time over 24 h

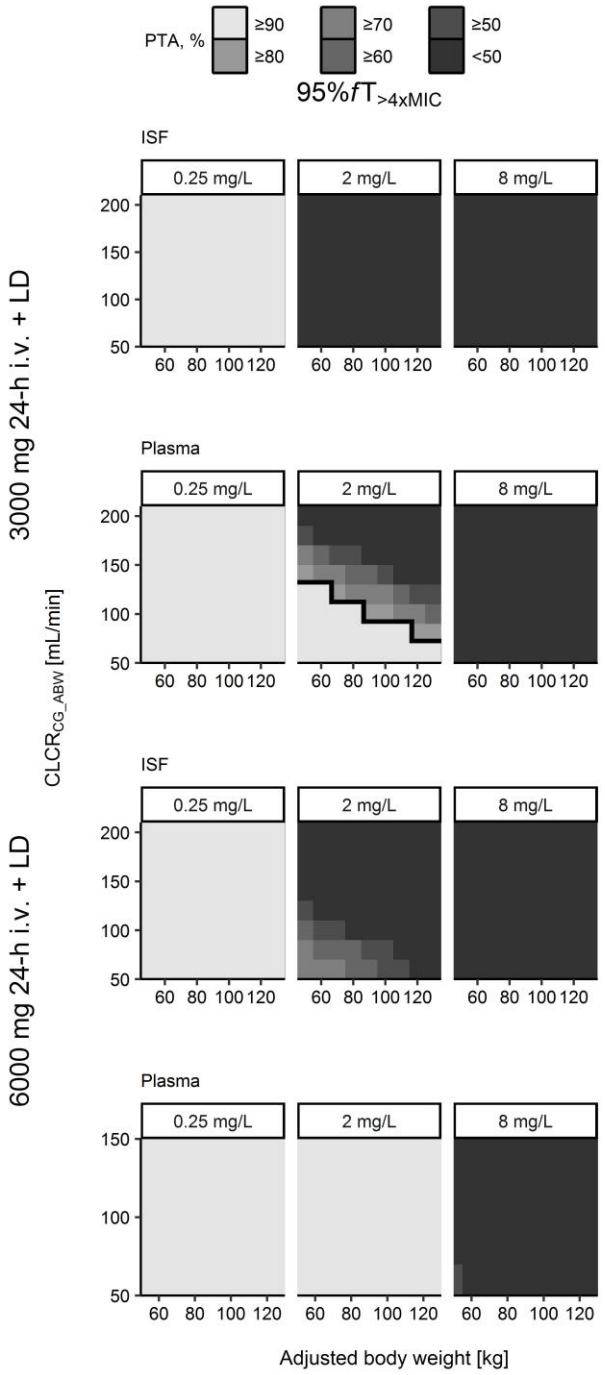

Fig. S14 Probability of target attainment versus adjusted body weight and serum creatinine clearance in plasma and ISF for 3000 mg (top) and 6000 mg (bottom) 24-h **continuous** infusion following a 30-min intravenous loading dose of 1000 mg (LD) and 95%$fT_{>4xMIC}$.

MIC is given at the top of each panel. Bold black lines separate PTA≥90% (adequate therapy, light grey) from PTA<90%.

Abbreviations: *ABW* adjusted body weight, $CLCR_{CG\_ABW}$ serum creatinine clearance calculated via Cockcroft-Gault equation based on ABW, *ISF* interstitial space fluid of the subcutaneous adipose tissue, *i.v,* intravenous, *MIC* minimum inhibitory concentration, *PTA* probability of target attainment, $95\%fT_{>MIC}$/$40\%fT_{>MIC}$ unbound meropenem plasma concentrations exceeding the MIC 95%/40% of the time over 24 h

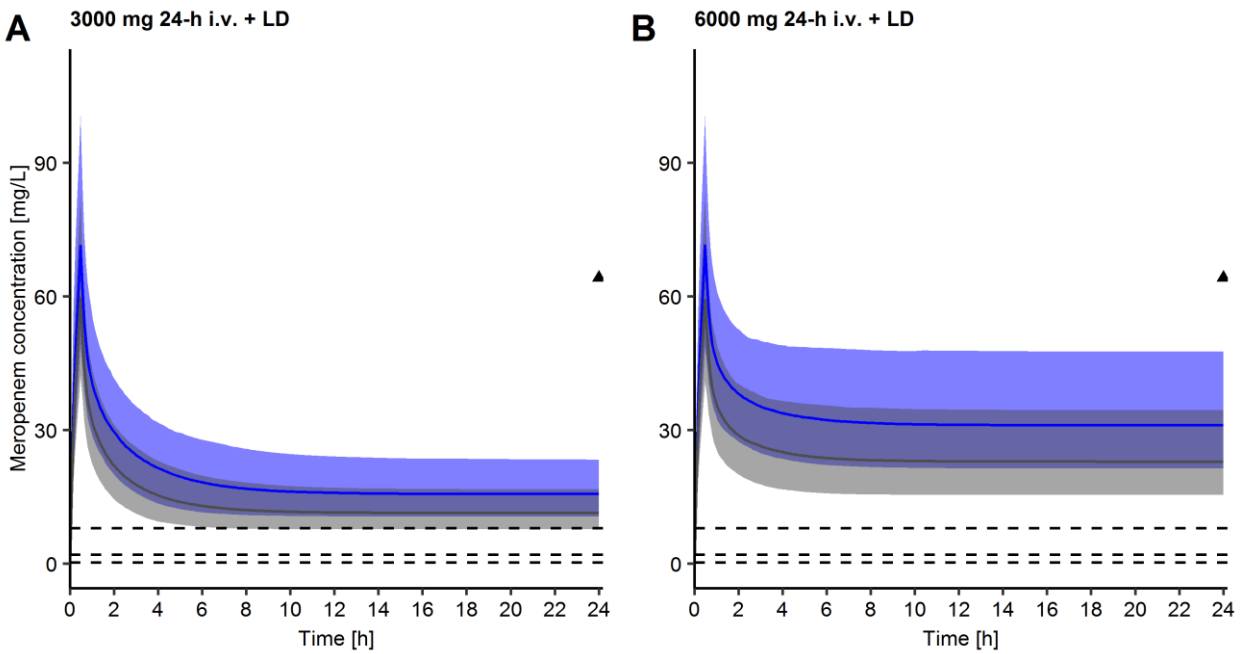

Fig. S15 Simulations of the meropenem concentration over time for a 6000 mg continuous intravenous infusion following a 1000 mg 30-min intravenous loading dose for an adjusted body weight of 60 kg and creatinine clearance of 60 mL/min (A) and a reference individual of 70 kg and 100 mL/min (B).
The 95% prediction interval is shaded in grey. The exemplary minimum inhibitory concentrations 0.25, 2 and 8 mg/L are shown as dashed horizontal lines. Triangles: Neurotoxicity thresholds for minimum plasma concentrations at steady-state reported by Imani et al. [2].

References

[1] Holford NHG, Anderson BJ. Allometric size: The scientific theory and extension to normal fat mass. Eur J Pharm Sci 2017;109:S59–64. doi:https://doi.org/10.1016/j.ejps.2017.05.056.

[2] Imani S, Marriott D, Buscher H, Sandaradura I, Gentili S. Too much of a good thing: a retrospective study of β-lactam concentration–toxicity relationships. J Antimicrob Chemother 2017;72:2891–7. doi:10.1093/jac/dkx209.